

Enhanced quasiparticle heat conduction of the multigap superconductor $\text{Lu}_2\text{Fe}_3\text{Si}_5$ Y. Machida,¹ S. Sakai,¹ K. Izawa,¹ H. Okuyama,² and T. Watanabe²¹*Department of Physics, Tokyo Institute of Technology, Meguro, Tokyo 152-8551, Japan*²*Department of Physics, College of Science and Technology,**Nihon University, Chiyoda, Tokyo 101-8308, Japan*

(Dated: October 11, 2018)

The thermal transport measurements have been made on the Fe-based superconductor $\text{Lu}_2\text{Fe}_3\text{Si}_5$ ($T_c \sim 6$ K) down to a very low temperature $T_c/120$. The field and temperature dependences of the thermal conductivity confirm the multigap superconductivity with fully opened gaps on the whole Fermi surfaces. In comparison to MgB_2 as a typical example of the multigap superconductor in a p -electron system, $\text{Lu}_2\text{Fe}_3\text{Si}_5$ reveals a remarkably enhanced quasiparticle heat conduction in the mixed state. The results can be interpreted as a consequence of the electronic correlations derived from Fe $3d$ -electrons.

PACS numbers: 74.25.fc, 74.70.Dd, 74.25.Op, 74.25.Jb

Multigap superconductivity (MGSC) is the existence of superconducting gaps with significantly different magnitude on distinct Fermi surfaces. This phenomena has been realized in wide variety of materials including MgB_2 [1], NbSe_2 [2] and the heavy fermions [3–5], pointing to its universality underlying the superconductivity. One consequence of the MGSC is the ability to excite low-energy quasiparticles (QPs) due to the presence of the small gap, providing unusual features in the mixed state. Even though the MGSC has been extensively studied so far, the purpose of the study has been mainly focused on the explanation for the anomalous properties observed in the superconducting state. Recent discovery of the iron-pnictide superconductors [6], however, have offered further insight into the MGSC especially in the correlated electron system because the electronic interactions and the multiband structure are essential for the pairing mechanism in this system [7]. In that sense, a question of how the electronic correlations affect on the MGSC is a fascinating issue to be addressed, which could not be examined on MgB_2 . Unfortunately, lack of high-quality stoichiometric samples and/or the high upper critical field prevent detailed studies of the MGSC in the iron-pnictides [7].

$\text{Lu}_2\text{Fe}_3\text{Si}_5$, a ternary-iron-silicide, is an another example of the Fe-based multigap superconductor with $T_c \sim 6$ K [8], which crystallizes in the tetragonal structure consisting of a quasi-one-dimensional iron chain along the c axis and quasi-two-dimensional iron squares parallel to the basal plane [9]. Band structure calculations predict that Fermi surfaces consist of two holelike bands and one electronlike band, and each band has a contribution from the Fe $3d$ -electrons [8]. In the two holelike bands, some parts of the Fermi surfaces have the different dimensionality reflecting the crystal structure [8]. Importantly, the Fe $3d$ -electrons are responsible for the superconductivity of $\text{Lu}_2\text{Fe}_3\text{Si}_5$, as suggested by the absence of superconductivity in the isoelectronic $\text{Lu}_2\text{Ru}_3\text{Si}_5$ and $\text{Lu}_2\text{Os}_3\text{Si}_5$ [10]. Therefore, $\text{Lu}_2\text{Fe}_3\text{Si}_5$

stands as the rare stoichiometric multigap superconductor with the d -electrons in between the p -electron system (e.g., MgB_2 [1]) and the f -electron system such as $\text{PrOs}_4\text{Sb}_{12}$ [3], providing an unique opportunity to study the MGSC in the moderately correlated electron system.

The multigap superconductivity of $\text{Lu}_2\text{Fe}_3\text{Si}_5$ is first observed by the specific heat measurement down to 0.3 K under zero field [8]. It is of interest to further elucidate the MGSC by performing the thermal conductivity measurements down to lower temperature in the vortex state, because the thermal conductivity is sensitive to the light carrier band which is expected to strongly affect on the low-energy QP excitations. Absence of the nuclear schottky contribution is another advantage of this technique in exploring the MGSC.

In this paper, we report on the thermal transport measurements of single crystalline $\text{Lu}_2\text{Fe}_3\text{Si}_5$ down to $T_c/120$. Our detailed results of the thermal conductivity in the mixed state confirm the MGSC in $\text{Lu}_2\text{Fe}_3\text{Si}_5$. Moreover, from a comparative study with MgB_2 , $\text{Lu}_2\text{Fe}_3\text{Si}_5$ reveals the significantly enhanced heat conduction as an indication of the electronic interactions derived from the Fe $3d$ -electrons.

Single crystals were grown by the floating-zone method [11]. One-heater-two-thermometer steady-state method was used to measure the thermal conductivity. The heat current q was aligned along the [001] direction, and the magnetic field is applied parallel to the ab plane. The thermal contacts with resistance of ~ 10 m Ω were made to the sample by using a spot welding technique.

Figure 1 shows the temperature dependence of the thermal conductivity divided by temperature $\kappa(T)/T$ under zero field. An arrow denotes the superconducting transition temperature $T_c \sim 6$ K. As clearly seen, $\kappa(T)/T$ shows a kink at T_c followed by steep decrease with decreasing temperature. On further cooling, a hump structure appears around 3 K. The decrease of $\kappa(T)/T$ in the superconducting state attributes to the reduction of the QP density by opening the superconducting gaps. On

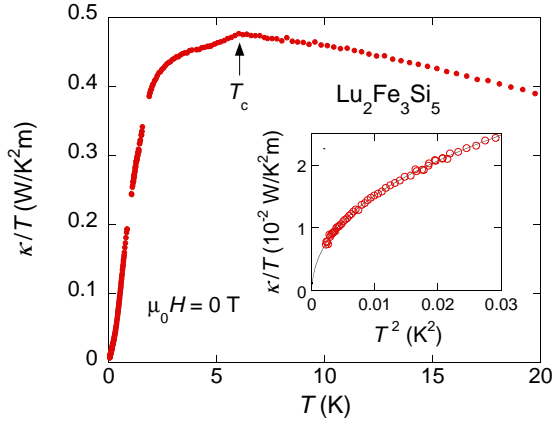


FIG. 1: (color online). Temperature dependence of the thermal conductivity divided by temperature κ/T under zero field. The arrow denotes the superconducting temperature T_c . Inset: κ/T vs. T^2 plot under zero field. The solid line represents a fit to the data by $\kappa/T = \kappa_0/T + bT^{\alpha-1}$.

the other hand, the hump structure originates from an enhanced phonon mean free path due to the condensation of electronic scattering centers in the superconducting state. In fact, similar enhancement of the phononic conductance (called phonon peak) in the superconducting state is also observed in various materials such as Nb [12] and Pb [13]. The inset of Fig. 1 shows κ/T vs. T^2 plot. Since the measured thermal conductivity contains both electron and phonon contributions, it is necessary to separate to each part as $\kappa = \kappa_e + \kappa_{ph}$. Below 0.15 K, κ/T is well described by a relation of $\kappa/T = \kappa_0/T + bT^{\alpha-1}$ with $\kappa_0/T = 0.000 \pm 0.005 \text{ W/K}^2\text{m}$, $b = 0.11 \text{ W/K}^{2.8}\text{m}$, and $\alpha \sim 1.8$. Here, we should note that the conventional T^3 dependence of the phonon thermal conductivity κ_{ph} dominated by the ballistic phonon scattering fails to reproduce our result. The lower power of κ_{ph} with $\alpha \sim 1.8$ can be attributed to either the specular reflection of the phonon or the phonon scattering off the electrons [14, 15]. For the electronic contribution, κ_0/T provides the electronic thermal conductivity in the zero temperature limit. The negligibly small κ_0/T clearly indicates that $\text{Lu}_2\text{Fe}_3\text{Si}_5$ is a fully gapped superconductor consistent with the specific heat measurement [8].

Figure 2 shows the field dependence of the thermal conductivity divided by temperature $\kappa(H)/T$ at several temperatures. For $T \geq 1.0$ K, $\kappa(H)/T$ takes a minimum at low fields and then increases with field. In general, the existence of the minimum of $\kappa(H)/T$ is explained as the result of the decrease of the phonon conductivity due to the vortex scattering concomitant with the increase of the electronic conductivity resulting from the increase of the delocalized QP density [2, 16, 17]. Remarkably, for $T < 1.0$ K, $\kappa(H)/T$ shows rapid increase and reaches almost half of the normal state value κ_n/T already at low fields ($\mu_0 H < 1$ T). Here, κ_n/T is estimated from the Wiedemann-Franz law via $\kappa_n/T = L_0/\rho_0 = 0.325$

$\text{W/K}^2\text{m}$, where $L_0 = 2.44 \times 10^{-8} \text{ W}\Omega/\text{K}^2$ is the Lorenz number, and $\rho_0 = 7.5 \mu\Omega\text{cm}$ is the normal-state residual resistivity. It is of interest to compare our results with several superconductors. The inset of Fig. 2 depicts the normalized thermal conductivity κ/κ_n at 0.1 K plotted against H/H_{c2} together with the data for Nb [17], MgB_2 [16], and UPt_3 [18]. Here, the phonon thermal conductivity $\kappa(H=0)$ is subtracted from κ/κ_n , and the upper critical field of $\mu_0 H_{c2} = 6.4$ T is obtained from Ref. [19]. The field variation of κ/κ_n for $\text{Lu}_2\text{Fe}_3\text{Si}_5$ is in dramatic contrast with the behavior of the fully gapped s -wave superconductor Nb [17], in which small magnetic fields hardly affect the low temperature thermal conductivity. By contrast, in nodal superconductor UPt_3 , the delocalized QPs induced by the Doppler shift produces the remarkable field dependence of κ/κ_n . The strongly enhanced thermal conductivity of $\text{Lu}_2\text{Fe}_3\text{Si}_5$ is a clear indication of either a gap with nodes or nodeless multiple gaps with significantly different magnitude on distinct Fermi surfaces. However, the nodal gap is ruled out by the absence of the T -linear term of $\kappa(T)$.

On the other hand, one immediately notices that $\text{Lu}_2\text{Fe}_3\text{Si}_5$ shares striking resemblance with MgB_2 , namely, a rapid increase of κ/κ_n at low fields and a saturation behavior at high fields, although κ/κ_n for $\text{Lu}_2\text{Fe}_3\text{Si}_5$ shows even more pronounced increase and takes higher values. The field evolution of the thermal conductivity of MgB_2 is well understood in terms of the multigap superconductivity with a small gap Δ_s on one Fermi surface and a large gap Δ_l on the other (index l and s represent large and small gaps, respectively) [16]. A consequence of the small gap is an existence of a “virtual upper critical field” H_{c2}^s , above which the overlap of huge vortex core provides a dramatic increase of the delocalized QPs contributed to the heat conduction.

The characteristic field scale of H_{c2}^s can be estimated from $H_{c2}^s/H_{c2} \sim (\Delta_s/\Delta_l)^2 (v_{F,l}/v_{F,s})^2$. On the other hand, the “normal state” contribution of the small gap band κ_s/κ_n is obtained from $\kappa_s/\kappa_n = \kappa_s/(\kappa_l + \kappa_s) = N_s v_{F,s}^2 \tau_s / (N_l v_{F,l}^2 \tau_l + N_s v_{F,s}^2 \tau_s)$ via a relation of $\kappa_i \propto N_i v_{F,i}^2 \tau_i$, where N_i , $v_{F,i}$, and τ_i represent the normal state electronic densities of state, the Fermi velocity, and the scattering rate of each gap band ($i = l, s$). Here, suppose τ_s/τ_l is close to unity, κ_s/κ_n is simplified to $\sim 1/\{1 + (N_l/N_s)(v_{F,l}/v_{F,s})^2\}$. Consequently, the two gap superconductivity is characterized by the three ratios Δ_l/Δ_s , N_l/N_s , and $v_{F,l}/v_{F,s}$. With the knowledge of $\Delta_l/\Delta_s \sim 4$ [1] and $N_l/N_s, v_{F,l}/v_{F,s} \sim 1$ [16], we find $H_{c2}^s/H_{c2} \sim 1$ and $\kappa_s/\kappa_n \sim 0.5$ for MgB_2 in agreement with various estimations [16, 20]. Now, let us discuss the case of $\text{Lu}_2\text{Fe}_3\text{Si}_5$. Since $\Delta_l/\Delta_s \sim 4$ and $N_l/N_s \sim 1$ [8] as same as MgB_2 , the κ/κ_n curve of $\text{Lu}_2\text{Fe}_3\text{Si}_5$ is expected to be scaled to that of MgB_2 by tuning the ratio of $v_{F,l}/v_{F,s}$. We achieve excellent scaling with $v_{F,l}/v_{F,s} \sim 0.8$ as shown by the open circles in the inset of Fig. 2, yielding $H_{c2}^s/H_{c2} \sim 0.04$ and $\kappa_s/\kappa_n \sim 0.6$. The devia-

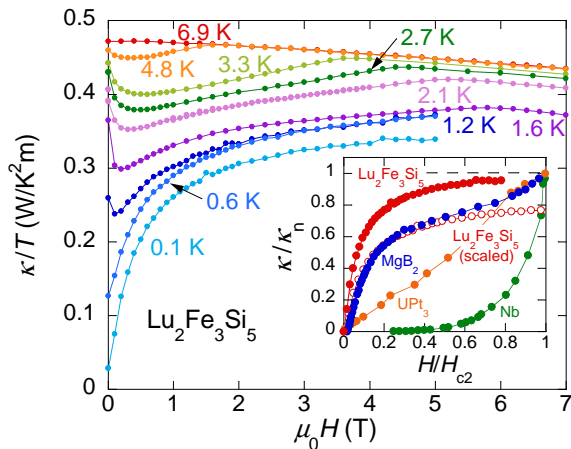


FIG. 2: (color online). Field dependence of the thermal conductivity divided by temperature κ/T at several temperatures. Inset: The thermal conductivity normalized to its normal state value κ/κ_n vs. H/H_{c2} plot at 0.1 K. For comparison, the data for Nb [17], MgB_2 [16], and UPt_3 [18] are also shown. The open circles show a result of scaling described in the text.

tion at high fields is due to the difference of H_{c2} in these two systems. The inequality of $v_{F,l}/v_{F,s}$ indicates that the carrier mass m , which is inversely proportional to v_F ($m \propto 1/v_F$), is different in each band for $\text{Lu}_2\text{Fe}_3\text{Si}_5$ in contrast to MgB_2 [16]. This contradiction might originate from the character of the dominant electrons contribute to the density of state at the Fermi surface; Fe $3d$ -electrons in $\text{Lu}_2\text{Fe}_3\text{Si}_5$ and B $2p$ -electrons in MgB_2 , respectively. In addition, unequal weight of the d character among the distinct Fermi surfaces yields the heavy and light carrier bands in $\text{Lu}_2\text{Fe}_3\text{Si}_5$. Notably, a signature of the electronic correlations possibly derived from the d -electrons can be found in the specific heat coefficient $\gamma_n = 23.7 \text{ mJ/molK}^2$ [8], which is about 10 times larger than that of MgB_2 ($\gamma_n = 2.62 \text{ mJ/molK}^2$) [21]. The rather small $\gamma_{\text{band}} = 8.69 \text{ mJ/molK}^2$ obtained from the band calculations [8] also indicates the presence of the electronic interactions. On the other hand, the small gap on the light carrier band provides dramatic enhancement of $\kappa(H)/T$ in the mixed state than that of MgB_2 because κ is sensitive to the light carrier mass.

In order to further clarify the multigap superconductivity of $\text{Lu}_2\text{Fe}_3\text{Si}_5$, we present the temperature dependence of $\kappa(T)/T$ in the vortex state (Fig. 3). By applying magnetic fields, we observe a pronounced increase of $\kappa(T)/T$ at low temperatures corresponding to the fast growth of $\kappa(H)/T$ at low fields. Furthermore, an anomaly associated with a slight change of slope is found around 0.8 K at 0.1 T, and it shifts to ~ 0.3 K at 0.25 T as denoted by the arrows in Fig. 3. With further increasing fields, the anomaly becomes more pronounced, being a maximum around 0.2 K above 1.0 T. The emergence of the maximum can be attributed to either the phononic

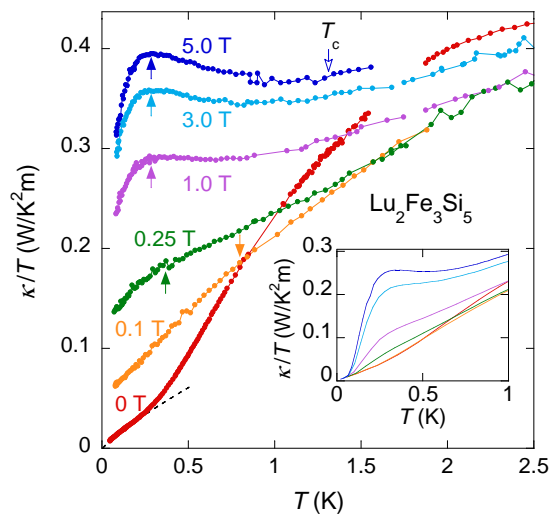


FIG. 3: (color online). Temperature dependence of the thermal conductivity divided by temperature κ/T under several magnetic fields. The solid and open arrows denote the anomalies associated with the small gap and T_c at 5 T, respectively. The dashed line represents a fit to the data by $\kappa/T = \kappa_0/T + bT^{-1}$. Inset: The calculated κ/T curves for the corresponding fields within the two-gap model described in the text.

or the electronic contribution. However, we immediately exclude the phononic origin because the appearance of phonon peaks twice below T_c is highly unlikely. Moreover, an increase of the phonon mean-free path up to 10 folds of the zero-field value, for example at 5 T, is improbable even if the low-temperature thermal conductivity is dominated by the specular reflection. Thus, we turn to the electronic origin raising the following possibilities; (1) an enhancement of the QP mean free path l_e , (2) a magnetic anomaly associated with a magnetic order, and (3) an increase of delocalized QPs excited above the field-suppressed small gap Δ_s . For the possibility of (1), the enhancement of l_e upon entering the superconducting state usually occurs as a result of the strong inelastic scattering. This is because normal state l_e suppressed by the inelastic scattering starts to increase in the superconducting state due to the condensation of electronic scattering centers. In practice, this behavior has been observed in CeCoIn_5 [22] and YBCO [23], in which a source of the inelastic scattering is attributed to the magnetic fluctuations. However, no signature of such magnetic fluctuation has been indicated in $\text{Lu}_2\text{Fe}_3\text{Si}_5$ [24]. The magnetic origin of the maximum is also ruled out because Fe atoms carry no magnetic moment [24]. Therefore, in the following we discuss the remaining possibility (3) by analyzing $\kappa(T)/T$ within the framework of the two-gap model.

In the superconducting state, the electronic thermal conductivity κ_e is expressed as,

$$\kappa_e/\kappa_n = \frac{2F_1(-y) + 2y\ln(1 + e^{-y}) + y^2(1 + e^y)^{-1}}{2F_1(0)}, \quad (1)$$

where $y = \Delta(t)/k_B T$, $\Delta(t)$ being the half of the energy gap and $t = T/T_c$ [25]. The temperature dependence of $\Delta(t)$ is given by standard gap interpolation formula $\Delta(t) = \Delta_0 \tanh(2.2\sqrt{1/t - 1})$, where Δ_0 is an energy gap at absolute zero. The term of $F_1(-y)$ is given by the expression $F_n(-y) = \int_0^\infty z^n (1 + e^{z+y})^{-1} dz$. Following the approach used for the specific heat [8], we generalize Eq.(1) to the two-gap model as $\kappa_e = n_s \kappa_{e,s} + (1 - n_s) \kappa_{e,l}$, where $\kappa_{e,i}$ ($i = l, s$) is the large and small gap bands thermal conductivity, respectively, and n_s is a weight for the small gap band. In the following analysis, n_s is fixed to be 0.6 regardless with the applied field, which is determined from the scaling. To obtain κ_n , we estimate the phonon thermal conductivity from the minima of $\kappa(H)/T$ shown in Fig. 2 assuming that the minima represent at most the maximum value of the phonon contribution [16].

The solid lines shown in the inset of Fig. 3 represent the calculated results of the total thermal conductivity $\kappa/T = \kappa_e/T + \kappa_{ph}/T$ based on the two-gap model at each field. Here, we assume the temperature dependence of the phonon thermal conductivity to be $\kappa_{ph}/T = 0.11 \times T^{0.8}$ as determined by the zero-field κ/T (the dashed line in Fig. 3). Moreover, at zero field, we use the gap values of $2\Delta_{0,l}/k_B T_c = 4.4$ and $2\Delta_{0,s}/k_B T_c = 1.1$ obtained from the specific heat measurement [8]. The field variation of $\Delta_l(H)$ is assumed to follow the mean-field description $\Delta_l(H) = \Delta_{0,l} \sqrt{1 - H/H_{c2}^s}$ (the solid line in Fig. 4). It should be emphasized that the two-gap model well reproduces the experimental results especially for the maximum of $\kappa(T)/T$ only by tuning the small gap $\Delta_s/k_B T_c$. The result further supports the existence of the small gap in $\text{Lu}_2\text{Fe}_3\text{Si}_5$. Furthermore, the maximum most likely originates from an increase of the delocalized QPs excited over the small gap. On the other hand, there exists a discrepancy between the experiment and the calculation below the maximum temperature; the experimental results show gradual decrease while the calculated κ/T rapidly drops to zero. One possible interpretation is that the system behaves like a dirty superconductor ($\xi > l_e$) due to the presence of $\mu_0 H_{c2}^s$ that gives rise to a large coherence length ξ . It has been argued that the superconductors in the dirty regime shows a rapid growth of QP density in the mixed state in comparison with those in the clean limit ($\xi \ll l_e$) [26].

The parameter of Δ_s/k_B obtained from the analysis and Δ_l/k_B are plotted against the magnetic field in Fig. 4. It is clearly seen that Δ_s/k_B sharply decreases at low field $\mu_0 H_s \leq 0.25$ T, while Δ_l/k_B shows monotonous decrease. Note that the characteristic field scale of $\mu_0 H_s$ is close to the virtual upper critical field $\mu_0 H_{c2}^s \sim 0.26$ T. Interestingly, a similar field-induced suppression of Δ_s below $\mu_0 H_{c2}^s$ is also observed in MgB_2 as demonstrated in the inset of Fig. 4, in which the gap values are determined by the point-contact study [27]. For the case of MgB_2 , this behavior is understood as a consequence of a weak interband pairing interaction [27, 28]. From the analogy

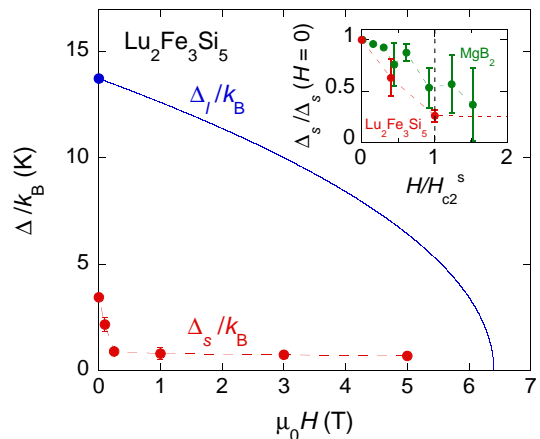


FIG. 4: (color online). Field dependence of the superconducting gaps Δ/k_B . Δ_l/k_B and Δ_s/k_B represent the large and small gaps, respectively. The solid line denotes the calculated result of Δ_l/k_B based on the mean-field description. The dashed line is a guide to the eye. Inset: The normalized small gap $\Delta_s/\Delta_s(H=0)$ vs. H/H_{c2}^s for $\text{Lu}_2\text{Fe}_3\text{Si}_5$ and MgB_2 [27].

of MgB_2 , the existence of the multiple bands having the different dimensionality and the weak interband interaction could be a source of the MGSC in $\text{Lu}_2\text{Fe}_3\text{Si}_5$.

In summary, our thermal conductivity measurements clarify the multigap superconductivity with a fully gapped excitation spectrum in $\text{Lu}_2\text{Fe}_3\text{Si}_5$. The weak coupling between the distinct gap bands is thought to be the origin of the multigap superconductivity. In contrast to MgB_2 , the dramatic enhancement of the quasiparticle heat conduction in the mixed state implies the presence of the electronic correlations derived from the Fe 3d-electrons. Our findings shed new light on the multigap superconductivity in the correlated electron systems.

We thank H. Harima, H. Kusunose, Y. Nakajima, and Y. Yanase for discussions. This work is supported by Grant-in-Aids for Scientific Research from JSPS and MEXT of Japan, and a Grant-in-Aid for the Global COE Program of the Tokyo Institute of Technology.

-
- [1] F. Bouquet et al., *Europhys. Lett.* **56**, 856 (2001).
 - [2] E. Boaknin et al., *Phys. Rev. Lett.* **90**, 117003 (2003).
 - [3] G. Seyfarth et al., *Phys. Rev. Lett.* **95**, 107004 (2005).
 - [4] Y. Kasahara et al., *Phys. Rev. Lett.* **99**, 116402 (2007).
 - [5] G. Seyfarth et al., *Phys. Rev. Lett.* **101**, 046401 (2008).
 - [6] Y. Kamihara et al., *J. Am. Chem. Soc.* **130**, 3296 (2008).
 - [7] K. Ishida, Y. Nakai, and H. Hosono, *J. Phys. Soc. Jpn.* **78**, 062001 (2009).
 - [8] Y. Nakajima et al., *Phys. Rev. Lett.* **100**, 157001 (2008).
 - [9] H. F. Braun, *Ternary Superconductors* (North-Holland, 1981), p. 225.
 - [10] D. C. Johnston and H. F. Braun, *Superconductivity Ternary Compounds II* (Springer-Verlag, 1982).

- [11] T. Watanabe et al., Phys. Rev. B **80**, 100502(R) (2009).
- [12] S. M. Wasim and N. H. Zebouni, Phys. Rev. **187**, 539 (1969).
- [13] M. H. Jericho, W. Odoni, and H. R. Ott, Phys. Rev. B **31**, 3124 (1985).
- [14] W. S. Hurst and D. R. Frankl, Phys. Rev. **186**, 801 (1969).
- [15] R. O. Pohl and B. Stritzker, Phys. Rev. B **25**, 3608 (1982).
- [16] A. V. Sologubenko et al., Phys. Rev. B **66**, 014504 (2002).
- [17] J. Lowell and J. B. Sousa, J. Low Temp. Phys. **3**, 65 (1970).
- [18] H. Suderow et al., J. Low Temp. Phys. **108**, 11 (1997).
- [19] Y. Nakajima et al., Physica C **469**, 921 (2009).
- [20] F. Bouquet et al., Phys. Rev. Lett. **89**, 257001 (2002).
- [21] H. J. Choi et al., Nature **418**, 758 (2002).
- [22] Y. Kasahara et al., Phys. Rev. B **72**, 214515 (2005).
- [23] Y. Zhang et al., Phys. Rev. Lett. **86**, 890 (2001).
- [24] H. F. Braun et al., J. Magn. Magn. Mater. **25**, 117 (1981).
- [25] J. Bardeen, G. Richayzen, and L. Tewordt, Phys. Rev. **113**, 982 (1959).
- [26] H. Kusunose, T. M. Rice, and M. Sigrist, Phys. Rev. B **66**, 214503 (2002).
- [27] R. S. Gonnelli et al., Phys. Rev. B **69**, 100504(R) (2004).
- [28] A. E. Koshelev and A. A. Golubov, Phys. Rev. Lett. **90**, 177002 (2003).